Optical transitions of Ho^{3+} ions in fluorozirconate glass

K. Tanimura, M. D. Shinn, and W. A. Sibley
Physics Department, Oklahoma State University, Stillwater, Oklahoma 74078

M. G. Drexhage and R. N. Brown
Rome Air Development Center, Hanscom Air Force Base, Bedford, Massachusetts 01731
(Received 12 December 1983; revised manuscript received 10 April 1984)

Optical-absorption and emission spectra are presented for Ho^{3+} ions in fluorozirconate (ZBLA) glass [the nominal composition of ZBLA glass (in mol%) is 57, ZrF_4; 34, BaF_2; 5, LaF_3; and 4, AlF_3]. The measured oscillator strengths and radiative rates for several transitions were compared with calculated values. Nonradiative transition rates for the excited states were determined by the difference between the measured rates and the calculated radiative rates. Multiphonon emission and energy-transfer effects accounted for the nonradiative transitions. The low-temperature multiphonon emission rates are in agreement with the rates predicted by the phenomenological energy-gap law, when one uses parameters obtained previously for ZBLA:Er^{3+}. The crystallization of ZBLA glass was studied, with Ho^{3+} and Er^{3+} ions as probes. Isochronal heating data indicate that the glass undergoes rapid devitrification around 630 K. The crystallization of ZBLA is found to involve two distinct processes.

I. INTRODUCTION

The discovery of fluoride glasses based primarily on zirconium or hafnium fluoride is quite recent.[1,2] Preparation of these glasses is straightforward and the resulting samples exhibit a wide range of transparency, extending from about 0.2 μm to 7 μm. This characteristic, along with an idex of refraction near 1.5 and good resistance to degradation from water or weak acids make these materials promising candidates for optical fibers.[3] The composition of the glasses is such that the trivalent lanthanides are easily incorporated, which may make these glasses good laser hosts.

At this time, studies on the optical properties of rare-earth ions in fluoride glasses have been on Nd^{3+},[4] Eu^{3+},[5] and Er^{3+}.[6–8] These investigations have shown that the inhomogeneous broadening of the emissions is narrower than that observed in oxide glasses. This is believed to be due to the ion's substitution into the less perturbed network-former sites.[4] Also, transitions between J manifolds which are normally absent or greatly quenched in oxide glasses are more intense in fluoride glasses. It has been presumed,[5–7] and explicitly shown,[8] that this arises from the low phonon energies ($\sim$500 cm^{-1}) of the fluoride glass hosts which reduce nonradiative transitions due to multiphonon emission.

The optical properties of Ho^{3+} have been studied in numerous crystalline and oxide glass hosts.[9–13] The purpose of this investigation is to study the optical properties of Ho^{3+} in fluorozirconate glass (ZBLA:Ho) to better understand the behavior of rare-earth ions in this host, and to augment our earlier results on ZBLA:Er.

II. EXPERIMENTAL METHODS

The samples used in this study were prepared at the Rome Air Development Center (RADC), Hanscom Air Force Base (AFB) laboratory using methods described earlier.[3] The starting composition (in mol%) was 57, ZrF_4; 34, BaF_2; 3, LaF_3; 4, AlF_3; and 2, HoF_3.

For low-temperature measurements, a Sulfrian helium cryostat, or a CTI Cryodyne Cryocooler Model 21SC was utilized. High-temperature measurements were made with the sample enclosed in a copper holder with small windows for the excitation and emission light. Temperature control was accomplished by using resistance heaters. Temperature control below room temperature was $\pm$1 K, while above room temperature it was $\pm$5 K.

Emission- and excitation-spectra measurements were made by exciting the samples with light from a 75-W xenon-arc lamp which had been passed through a 0.22-m Spex monochromator. The fluorescence was focused into a 0.8-m Spex monochromator, and a mirror was used to route the light emerging from the exit slit to the appropriate detector. These detectors were a cooled RCA C31034 photomultiplier tube (PMT) for the visible and a cooled Optoelectronics OTC-22-53 PbS cell for the infrared. The emission monochromator and PMT response was corrected by using a quartz-iodine lamp traceable to the National Bureau of Standards. The signal from the detector was preamplified and passed to a lock-in amplifier whose reference was a variable-speed light chopper in the excitation beam. The output of the lock-in may be displayed on an X-Y recorder or stored by a Hewlett-Packard HP-85 mincomputer.

Lifetime measurements were made utilizing a Biomation 610B transient recorder and a Nicholet 1070 signal averager. This system allowed lifetimes as short as 10 μs to be measured. For all lifetime measurements, except the $^5I_6$ and $^5I_7$ levels, the flourescing level was directly excited. For the $^5I_6$ and $^5I_7$ levels the $^5F_5$ level was excited. This was found to result in a faster signal acquisition time with no measureable change in lifetime.

Optical-absorption measurements were made with the

 ©1984 The American Physical Society

use of a Perkin-Elmer 330 spectrophotometer. At all times the spectral resolution was much greater than the observed linewidths. Integrated intensities were calculated by numerical integration.

III. EXPERIMENTAL RESULTS

The absorption spectrum of the 2.0 at. % Ho^{3+} sample was measured in the range from 250 to 2600 nm. The oscillator strengths (f) of the absorption transitions were calculated using the equation

$$f=\frac{mc}{\pi e^2 N}\int \alpha(\nu)d\nu\,, \tag{1}$$

where N is the number of ions per cm^3 and α is the absorption coefficient. All transitions were assumed to be electric dipole in nature, except for the $^5I_8\rightarrow{}^5I_7$ transition, which has a substantial magnetic dipole component. The values are presented in Table I. Values for Ho^{3+} in several other hosts are shown for comparison. The value for N, the concentration, was taken to be equal to the concentration in the starting mixture. This has been found to be accurate for previous rare-earth dopings of fluoride glasses. In several instances where levels of different J manifolds overlap, the unresolved intensity was assigned to the group of levels. The average frequencies $\bar{\nu}$ of the transitions were taken to be the centers of gravity of the absorption bands.

The magnitude of the measured oscillator strengths of many trivalent rare earths in solids and solutions has been calculable from the theory put forth independently by Judd[14] and Ofelt.[15] The assumptions of the theory were well described earlier;[14–18] therefore, only those formulas needed for application of the theory will be presented.

In the Judd-Ofelt theory, the electric dipole oscillator strength of a transition of average frequency $\bar{\nu}$ from a level J to the level J' is

$$f(a,J;b,J')=\left[\frac{8\pi^2 m\bar{\nu}}{3h(2J+1)e^2n^2}\frac{n(n^2+2)^2}{9}\right]\times S_{\mathrm{ED}}(a,J;b,J')\,, \tag{2}$$

where n is the refractive index of the medium, and S_{ED} is the electric dipole line strength,

$$S_{\mathrm{ED}}(a,J;b,J')=e^2\sum_{t=2,4,6}\Omega_t(\langle f^N J||U^{(t)}||f^N J'\rangle)^2\,. \tag{3}$$

In Eq. (3) the Ω_t are phenomenological parameters to be determined for the particular ion-host combination, and the squared terms are the matrix elements of the doubly reduced unit tensor $U^{(t)}$ for the rare-earth ion, whose intermediate-coupled eigenstate is represented by $|f^N J\rangle$.[19] The matrix elements calculated by Weber *et al.* for Ho^{3+} in LaF_3 were used.[9,20] This is a reasonable approximation, since the matrix elements are almost host invariant.[6,17] By substituting Eq. (3) into Eq. (2) and using the experimentally determined values of the oscillator strengths of the various observed transitions (Table I), a least-squares-fitting approach was used to find the Ω_t parameters. The variation in n with transition wavelength was well accounted for by using Cauchy's relation[8] with $n=A+B/\lambda^2$, with $A=1.505\,83$ and $B=3478.14\ \mathrm{nm}^2$.

Since magnetic dipole transitions make a large contribution to the $^5I_8\rightarrow{}^5I_7$ oscillator strength, this transition was deleted in fitting the Judd-Ofelt parameters. The parameters are $\Omega_2=2.28\times10^{-20}\ \mathrm{cm}^2$, $\Omega_4=2.08\times10^{-20}\ \mathrm{cm}^2$, and $\Omega_6=1.73\times10^{-20}\ \mathrm{cm}^2$. The calculated oscillator strengths are presented in Table II. A measure of the quality of the fit can be noted from the rms deviation δ_{rms} between the measured and calculated oscillator strengths

$$\delta_{\mathrm{rms}}=\left[\frac{\sum(\Delta f)^2}{N_{\mathrm{transition}}-N_{\mathrm{param}}}\right]^{1/2}, \tag{4}$$

TABLE I. Measured oscillator strengths of Ho^{3+} in various hosts at 300 K. All transitions are from the $^5I_8$ level to the levels indicated.

Level	Oscillator strength (10^{-8})				
	ZBLA	LaF_3[a]	$YA10_3$[a]	Germanate glass[b]	Tellurite glass[b]
$^5I_7$	144.0	68.0	128.0	90.0	208.0
$^5I_6$	72.0	36.0	64.0	26.0	115.0
$^5I_5$	11.6	6.2	12.0		28.0
$^5I_4$	1.5		4.0		
$^5F_5$	267.4	131.0	217.0	124.0	470.0
$^5S_2$, $^5F_4$	355.4	140.0	270.0	158.0	640.0
$^5F_3$, $^5F_2$, $^3K_8$	235.8	93.0	174.0	98.0	422.0
$^5G_6$	1045.6	436.0	745.0	2403.0	3577.0
$^5G_5$	231.9	110.0	210.0	136.0	531.0
$^5G_4$, $^3K_7$	47.4	21.0	51.0	45.0	
$^5G_2$, $^3H_5$, $^3H_6$	337.1	148.0	252.0	557.0	
$^5G_3$, $^3L_9$	54.9	25.0	49.0		
$^3F_4$, $^3K_6$, $^3D_2$	62.6	31.0	54.0	78.0	
$^3G_3$, $^3L_8$, $^3M_{10}$, $^5D_4$	273.5	120.0	260.0		
$^3F_2$, $^3H_4$	215.0	106.0	173.0		

[a]Reference 9.
[b]Reference 12.

TABLE II. Calculated oscillator strengths of Ho^{3+} in ZBLA glass. All transitions are from the $^5I_8$ level to the levels indicated.

Level	Oscillator strength (10^{-8}) Wavelength (nm)	Oscillator strength	Residual
$^5I_6$	1163	96	−24
$^5I_5$	894	18	−6
$^5I_4$	753	1.5	0
$^5F_5$	643	252	15
$^5S_2$, $^5F_4$	537	341	14
$^5F_3$, $^5F_2$, $^3K_8$	478	240	−4
$^5G_6$	450	1053	−7
$^5G_5$	416	233	−1
$^5G_4$, $^3K_7$	384	49	−2
$^5G_2$, $^3H_5$, $^3H_6$	360	296	41
$^5G_3$, $^3L_9$	345	87	−32
$^3F_4$, $^3K_6$, $^3D_2$	332	74	−11
$^3G_3$, $^3L_8$, $^3M_{10}$, $^5D_4$	287	309	−36
$^3F_2$, $^3H_4$	277	190	25

where $\sum(\Delta f)^2$ is the sum of squares of deviations, $N_{\text{transition}}$ is the number of transitions, and N_{param} is the number of parameters. The rms deviation is 0.23×10^{-6}, which is comparable to the rms deviations found by applying the Judd-Ofelt theory to rare-earth ions in other systems.

The forced electric dipole transition probabilities for excited states were calculated from the equation

$$A(a,J;b,J')=\frac{64\pi^4\bar{\nu}^3}{3(2J+1)hc^3}\frac{n(n^2+2)^2}{9}S_{\text{ED}} . \quad (5)$$

From these values it is possible to calculate the radiative lifetime τ of an excited state i,

$$\frac{1}{\tau_i}=\sum_j A(i,j) , \quad (6)$$

where the summation is over electric and magnetic dipole transitions to all terminal states j and the branching ratio

$$\beta=\frac{A(i,j)}{\sum_j A(i,j)}=\tau_i A(i,j) . \quad (7)$$

The values of A, τ, and β for the various transitions are given in Table III. For the $^5I_7\rightarrow{}^5I_8$ transition the total spontaneous transition probability (electric—plus—magnetic-dipole) was found using the relation[21,22]

$$A(a,J;b,J')=\frac{8\pi n^2\bar{\nu}^2}{c^2}\frac{2J'+1}{2J+1}\int\sigma(\nu)d\nu \quad (8)$$

to be equal to 64 s^{-1}.

The emission spectra of Ho^{3+} at 300 and 14 K are shown in Figs. 1(a) and 1(b), respectively. In both cases the excitation was at 288 nm. For all the emission lines shown in the figure the excitation spectra were measured. Based on these spectra, and the energies of the J manifolds obtained by absorption measurements, the fluorescent transitions were assigned. In Fig. 1 the line marked by an asterisk is due to the transition $^5F_3\rightarrow{}^5I_8$ and the line marked by a plus is due to the transition $^5G_4\rightarrow{}^5I_8$; other emission assignments are given in Table III.

Five emissions were observed due to transitions from the $^3P_1(^3D_3)$ level to lower excited states. In Table III calculated and experimentally determined branching ratios are compared. The average relative error is about 20%.

When samples were warmed from 14 K to room temperature, it was found that the emission at $\sim18\,300$ cm^{-1} (546 nm) broadens considerably (Fig. 1). The broadening arises from an increase in intensity of the high-energy side of the emission. This increase is due to thermalization of the $^5F_4$ level by the $^5S_2$ level, with the former level having a larger transition probability to the $^5I_8$ ground state (Table III). The transition rate of the $^5F_4\rightarrow{}^5I_7$ emission is much lower than the $^5S_2\rightarrow{}^5I_7$ emission (Table III) so insignificant broadening occurs for their combined emissions, at $\sim13\,300$ cm^{-1} (725 nm) (Fig. 1). In order to determine the energy gap E between these two levels the ratio of the $^5S_2(^5F_4)\rightarrow{}^5I_7$ emission intensity (I_7) to the $^5S_2(^5F_4)\rightarrow{}^5I_8$ emission intensity (I_8) is plotted as a function of temperature in Fig. 2. An analysis based on a four-level system comprised of the $^5F_4$ (level 1), $^5S_2$ (level 2), $^5I_7$ (level 3), and $^5I_8$ (level 4) J manifolds predicts that the ratio I_7/I_8 is[8]

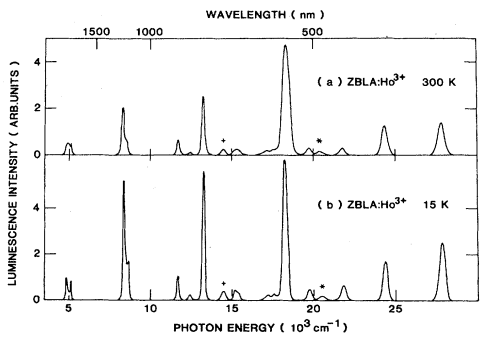

FIG. 1. Emission spectra of Ho^{3+} in ZBLA glass at (a) 300 K and (b) 15 K. The symbols above the bands are explained in the text.

TABLE III. Predicted spontaneous-emission probabilities of Ho^{3+} in ZBLA glass. Included are the predicted and measured branching ratios for the $^3P_1$ ($^3D_3$) level.

Transition	Average frequency (cm^{-1})	A_{ED} (s^{-1})	τ_R (ms)	Branching ratios Calculated	Measured
$^5I_7 \rightarrow {}^5I_8$	5092	57.7		1.00	
$^5I_6 \rightarrow {}^5I_8$	8596	140.3	6.5	0.91	
$^5I_7$	3504	14.3		0.09	
$^5I_5 \rightarrow {}^5I_8$	11186	51.7	7.8	0.40	
$^5I_7$	6094	72.3		0.56	
$^5I_6$	2590	5.0		0.04	
$^5I_4 \rightarrow {}^5I_8$	13273	7.8	12.5	0.10	
$^5I_7$	8181	37.5		0.47	
$^5I_6$	4677	30.4		0.38	
$^5I_5$	2087	4.2		0.05	
$^5F_5 \rightarrow {}^5I_8$	15547	1435.7	0.54	0.77	
$^5I_7$	10455	341.1		0.18	
$^5I_6$	6951	77.0		0.04	
$^5I_5$	4361	6.0			
$^5I_4$	2274	4.5			
$^5S_2(^5F_4) \rightarrow {}^5I_8$	18608	1144.2(2790.7)	0.47(0.18)	0.54(0.82)	
$^5I_7$	13516	782.0(287.9)		0.37(0.08)	
$^5I_6$	10012	138.1(206.4)		0.07(0.06)	
$^5I_5$	7422	34.9(109.0)		0.02(0.03)	
$^5I_4$	5335	36.3(18.5)		0.02	
$^5F_5$	3061	0.4(4.6)			
$^3P_1+{}^3D_3 \rightarrow {}^5I_8$	32942	55.2	0.20	0.01	
$^5I_7$	27850	1987.6		0.39	0.39
$^5I_6$	24346	1660.4		0.33	0.32
$^5I_5$	21756	220.3		0.04	0.07
$^5I_4$	19669	226.5		0.05	0.06
$^5F_5$	17395	54.1		0.01	
$^5S_2$, $^5F_4$	14334	121.0		0.02	
$^5F_3$	12264	138.4		0.03	
$^3K_8$	11501	317.8		0.06	0.08
$^5G_6$	10705	11.6			
$^5G_5$	8909	158.3		0.03	
$^5G_4$, $^3K_7$	6934	37.0			
$^3H_6$	5133	66.8		0.01	

$$\frac{I_7}{I_8}=\frac{C_7(\nu)h\nu_7}{C_8(\nu)h\nu_8}\frac{9A_{42}e^{-E/kT}+5A_{32}}{9A_{41}e^{-E/kT}+5A_{31}}, \tag{9}$$

where A_{ij} is the probability for a spontaneous transition between levels i and j, and $C_7(\nu)$ and $C_8(\nu)$ represent the response of the detection system in the frequency range of I_7 and I_8, respectively. At low tempreatures ($E \gg kT$) this equation gives the ratio of the $^5S_2 \rightarrow {}^5I_7$ and $^5S_2 \rightarrow {}^5I_8$ transition rates. With the use of the values from Table III, Eq. (9) yields the ratio $I_7/I_8=0.68$ for $T \approx 0$. This value agrees with the experimentally determined value of 0.67 at low temperatures. The solid curve in Fig. 2 is the result of substituting the calculated transition rates from Table III and a value of $E=90$ cm^{-1} in Eq. (9). The value obtained is in agreement with the $^5S_2$, $^5F_4$ splittings observed in other hosts.[11,23]

The temperature dependence of the lifetimes of the J manifolds $^3P_1(^3D_3)$, $^5S_2(^5F_4)$, $^5F_5$, $^5I_6$, and $^5I_7$ are shown in Figs. 3–6. Although luminescence was detected from the $^5G_4$ and $^5F_3$ levels, the lifetimes were too fast to measure. The errors in these measurements are estimated to be ~5%. The decays of the measurable transitions, except the $^5S_2(^5F_4)$ emission, could be fitted to a single ex-

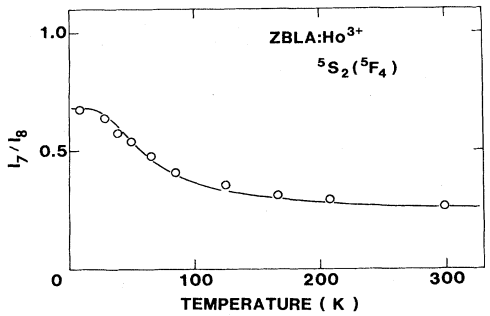

FIG. 2. Ratio of the intensities of the $^5S_2(^5F_4) \rightarrow {}^5I_7(I_7)$ and $^5S_2(^5F_4) \rightarrow {}^5I_8(I_8)$ emissions as a function of temperature.

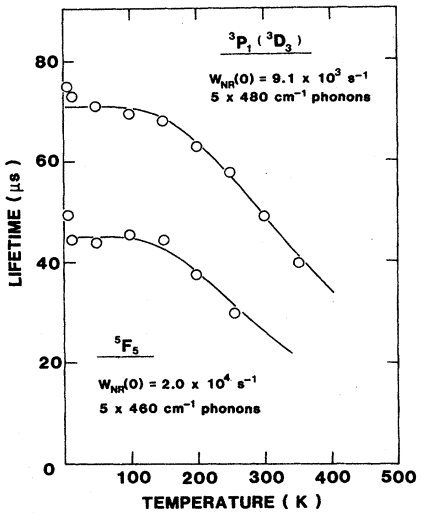

FIG. 3. Temperature dependence of the $^3P_1(^3D_3)$ and $^5F_5$ emission lifetimes.

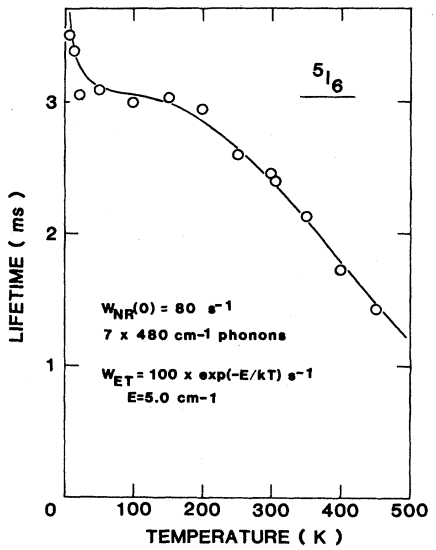

FIG. 5. Temperature dependence of the $^5I_6$ emission lifetime.

ponential. The decay of the $^5S_2(^5F_4)$ emission was nearly single exponential, with a ratio between the first and third e-folding time of ≥ 0.80. For this transition the first e-folding time was used as the value for the lifetime.

Changes in optical properties of rare-earth ions can be utilized as a probe to study the crystallization of ZBLA glass. Isothermal and ischronal devitrification experiments were performed on 2 mol% Er^{3+}-doped ZBLA samples used in Ref. 8. The emission from the $^4S_{3/2} \rightarrow {}^4I_{15/2}$ transition was measured at 15 K after each stage of thermal treatment. For the isochronal devitrification experiments the sample was kept at a fixed temperature for 15 min and then quenched. As the sample was heated to successively higher temperatures, the inhomogeneously broadened emission was replaced by a number of resolvable lines, with relative intensities similar to those observed in $RbMgF_3$:Er.[24] After each temperature treatment, the spectrum obtained was deconvoluted into two components. One is the luminescence characteristic of Er^{3+} in ZBLA glass, shown as spectrum (a) in Fig. 7. The other is the luminscence of Er^{3+} in the devitrified fraction of ZBLA glass, shown as spectrum (b) in the same figure. Also shown is the ratio of the luminescence intensity of the devitrified glass to the total intensity, plotted as a function of temperature. The fraction of devitrified material increases markedly at 630 K. This temperature is somewhat lower than the crystallization temperature reported from analysis of differenital scanning calorimetry (DSC) and differential thermal analysis (DTA) measurements.[3,4] Measurements similar to those described above were also performed on ZBLA:Ho. After heating a sample to 615 K for 10 h and remeasuring its emission spectrum, only slight changes were observed. This indicates that the Stark splitting of the J manifolds is less for Ho^{3+} than for Er^{3+}.

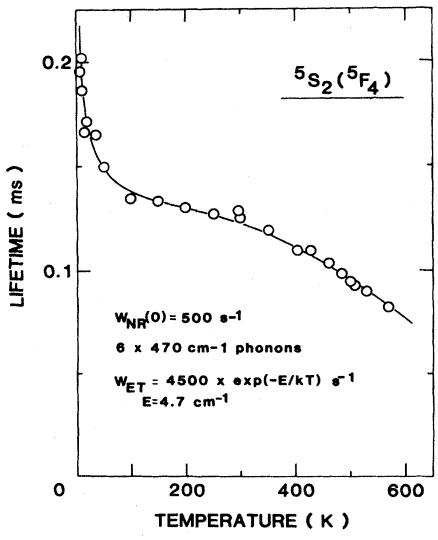

FIG. 4. Temperature dependence of the $^5S_2(^5F_4)$ emission lifetime.

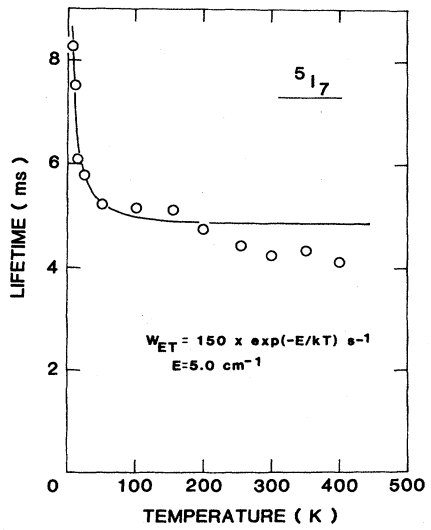

FIG. 6. Temperature dependence of the $^5I_7$ emission lifetime.

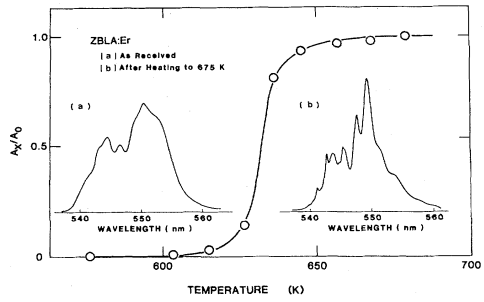

FIG. 7. Ratio of the Er^{3+} $^4S_{3/2}\rightarrow{}^4I_{15/2}$ emission intensity from the devitrified fraction of ZBLA glass (A_x) to the total intensity (A_0), as a function of temperature. The spectra shown are the emissions (a) before and (b) after devitrification.

For isothermal devitrification experiments the same procedure was used to determine the fraction of the sample which had devitrified. This is plotted as a function of heating time, for two different temperatures, in Fig. 8. Note the initial delay, whose magnitude depends on the temperature, followed by a period in which the devitrification occurs. In addition to the emission fluorescence measurements described previously, decay measurements were also made at 15 K on a devitrified sample of ZBLA:Er. Before treatment the decay was almost single exponential, with a first e-folding time of 600 μs.[8] After devitrification the decay was single exponential with a lifetime of 460 μs. The single-exponential decay indicates that the rare-earth ion occupies one-site symmetry in the devitrified host.

IV. DISCUSSION

The magnitude of the nonradiative transitions from the various emitting states of Ho^{3+} in ZBLA is important for determining the radiative efficiency. The radiative efficiency η can be determined from the lifetime and radiative rate of the state in question and the equation

$$\eta=\tau W_{\text{rad}} , \tag{10}$$

where τ is the measured lifetime

$$\frac{1}{\tau}=W_{\text{rad}}+W_{\text{nonrad}} . \tag{11}$$

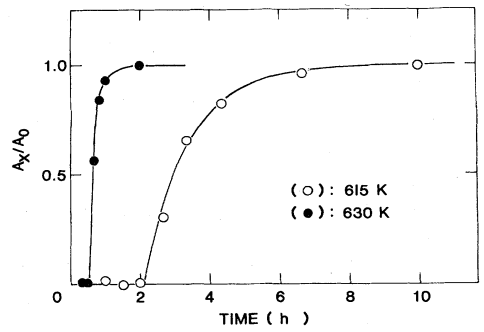

FIG. 8. Ratio of the emission intensity from the devitrified fraction of ZBLA glass (A_x) to the total intensity (A_0) as a function of time at temperatures of 615 K (open circles) and 630 K (solid circles).

W_{rad} is the radiative rate of the state, and W_{nonrad} is the nonradiative rate. The nonradiative rate can be further defined as the sum of W_{NR} and W_{ET}, which are the nonradiative rates due to multiphonon emission and energy transfer, respectively. For low rare-earth ion concentrations $W_{\text{ET}}\cong 0$, which allows nonradiative rates due to multiphonon emission to be determined directly. Previous work[4] on ZBL:Nd indicated that concentration quenching is significant for concentrations above 1 at.%. In ZBLA:Er, lifetime quenching was observed when the concentration was increased from 0.5 to 2.0 at.%.[8] The most pronounced effect noted was a rapid decrease in lifetime as the temperature was raised above 10 K. This type of decrease is also apparent in Figs. 3–6.

In order to determine the functional dependence of W_{ET} on temperature, the lifetime of the $^4S_{3/2}\rightarrow{}^4I_{15/2}$ transition for both concentrations of ZBLA:Er was measured over a narrow temperature range. It has been shown[8] that the multiphonon emission rate is negligible for this level. By subtracting the inverses of the lifetimes of the 0.5% sample from the 2% sample, the energy-transfer rate at that temperature is found. Figure 9 is a semilogarithmic graph of W_{ET} versus inverse temperature. The results for Er^{3+} are shown as open circles. The data indicated an exponential dependence on inverse temperature, from which it follows that W_{ET} can be described by

$$W_{\text{ET}}=W_{\text{ET}}(0)\exp(-E/kT) . \tag{12}$$

The values obtained from the best fit to the data are $W_{\text{ET}}(0)=87\ \text{s}^{-1}$ and $E=33\ \text{cm}^{-1}$.

A negligible multiphonon emission rate would be expected for the $^5I_7$ state; yet, a considerable increase in lifetime below 20 K is evident in Fig. 6. The calculated radiative rate for this level was subtracted from the inverse of the lifetime at each temperature. The difference is plotted as the circles in Fig. 10. Again, Eq. (12) may be applied to this data. The solid line, which represents the best fit, is given by $W_{\text{ET}}(0)=150\ \text{s}^{-1}$ and $E=5.0\ \text{cm}^{-1}$. For the $^3P_1(^3D_3)$ and $^5F_5$ decays, the sharp drop in the values of the lifetime below 50 K is small, so energy-transfer pro-

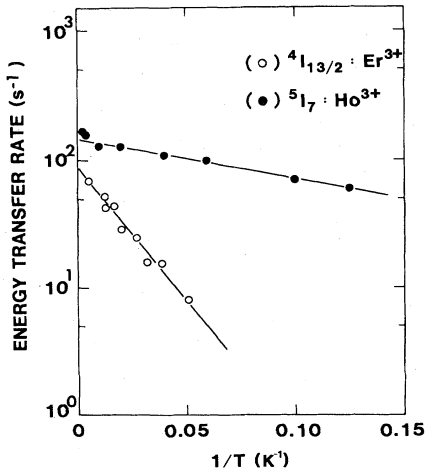

FIG. 9. Energy-transfer rate of the Er^{3+} $^4I_{13/2}\rightarrow{}^4I_{15/2}$ and Ho^{3+} $^5I_7\rightarrow{}^5I_8$ emissions as a function of inverse temperature.

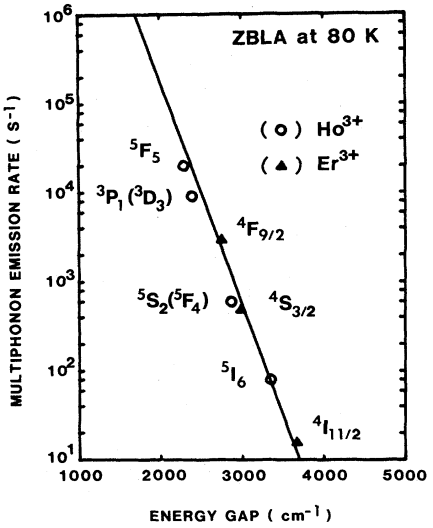

FIG. 10. Multiphonon emission rates of Er^{3+} (Ref. 8) and Ho^{3+} in ZBLA glass at 80 K as a function of the energy gap to the next lower level.

cesses are neglected. The $^5I_6$ level also shows the sharp decrease in lifetime and then a fairly constant lifetime until ~ 150 K. This is indicative of a low activation energy and thus for simplicity a constant value of $W_{ET}(0)=100$ s^{-1} was used. For the $^5S_2(^5F_4)$ levels the situation is more complicated, due to the thermalization of these levels. The effective radiative rate of the transition is[6,8]

$$\frac{1}{\tau_{\text{eff}}}=\frac{9\sum_i A(^5F_4)e^{-90/kT}+5\sum_i A(^5S_2)}{9e^{-90/kT}+5} . \tag{13}$$

With the use of the values of the radiative rates (Table III) and the calculated value of $E=90$ cm^{-1}, the effective radiative rate was determined. When subtracted from the inverse of the lifetime below 50 K, the remainder could be fitted by Eq. (12), with $W_{ET}(0)=4500$ s^{-1} and $E=4.7$ cm^{-1}.

It is interesting that an expression such as Eq. (12) can fit the temperature dependence of the energy transfer so well. One explanation lies in the thermalization of higher-energy Stark levels of the J manifold. In glass, the different site symmetries cause a lowering of the resonance between the Stark levels of adjacent ions. This decreases the probability of energy transfer.[25,26] Thermalization of the higher-energy Stark levels may remove this mismatch, resulting in an enhanced energy-transfer rate. A second possibility is a multistep diffusion type of energy transfer that involves resonant two-phonon-assisted processes. The theoretical expression for such a process contains a Boltzmann population term which dominates the temperature dependence of the energy-transfer rate.[27] Further study will be required before the physical significance of the value of E in Eq. (12) is understood. Here it will be treated as an empirical parameter.

Several expressions have been shown to adequately account for the temperature dependence of the multiphonon emission rate.[8] These expressions are based on the assumption that phonons of a single energy $\hbar\omega$ are active in the transition. The most commonly used expression, the single-frequency phonon model, developed by Riseberg and Moos is[28]

$$W_{\text{NR}}=W_{\text{NR}}(0)\left[\frac{\exp(\hbar\omega)}{\exp(\hbar\omega)-1}\right]^p , \tag{14}$$

where p is the number of phonons required to span the energy gap between adjacent levels, and $W_{\text{NR}}(0)$ is the low-temperature multiphonon emission rate. It has been shown that the energy of the phonons active in the nonradiative transition is about 460–500 cm^{-1}. This value is consistent with the highest-energy phonons present in the ZBLA host.[8,29] The observed multiphonon emission rates for the $^3P_1(^3D_3)$, $^5S_2(^5F_4)$, $^5F_5$, and $^5I_6$ levels were calculated from Eq. (11) by using the radiative rates predicted by the Judd-Ofelt theory, the fitted values of the energy transfer, and the measured lifetimes. Because of inhomogeneous broadening, the energy gaps cannot be explicitly known. However, it is possible to establish reasonable limits on the gap values from the absorption and emission spectra. The initial values of p and $\hbar\omega$ calculated from the relation $p=E/\hbar\omega$ and substituted into Eq. (14). These values, along the value of $W_{\text{NR}}(0)$, were adjusted to give the best fit to the observed rate. The final values are shown in Figs. 3–6. Note that the values of $\hbar\omega$ are in the range found previously.[8] With the use of the calculated multiphonon emission, energy transfer, and radiative rates in Eq. (11), the calculated lifetimes were determined. They are shown as solid lines in the figures. It should be noted that the multiphonon emission rate predicted for the $^5I_7$ transition was very low ($\ll 1$ s^{-1}) at all temperatures of interest. The line drawn in Fig. 6 is thus the sum of the calculated radiative and energy-transfer rates.

Another expression for the temperature dependence of the nonradiative rate was developed by Huang and Rhys.[30] Their theory is also based on the assumption of interactions with single-frequency phonons. It can be shown that their expression is identical to Eq. (14) except for a multiplicative factor $\exp(-2nS_0)$, where S_0 is the Huang-Rhys factor[8] and n is the phonon occupation number ($n=[\exp(\hbar\omega/kT)-1]^{-1}$) if S_0 is small. For rare-earth ions, S_0 is typically no greater than 0.1,[8,31] which makes $\exp(-2nS_0)$ change from unity at low temperatures to 0.92 at 600 K, for a phonon energy of 500 cm^{-1}. It was shown previously that this was indeed the case when both models were used to fit the same data.[8]

It has been noted[8] that in using the single-frequency phonon model [Eq. (14)] the validity of the $W_{\text{NR}}(0)$ values obtained experimentally should be checked. This can be accomplished by applying an approximation of the Huang-Rhys expresssion shown below, which is valid for small S_0 and $T=0$:[8,31]

$$W_{\text{NR}}(0)=N\exp(-S_0)S_0^p/p! , \tag{15}$$

where N is a constant on the order of 10^{13} s^{-1}, and p is again the number of phonons involved in the transition. Because of the inhomogeneous broadening of the Ho^{3+} luminescence and absorption bands in the host, it is practically impossible to estimate the magnitude of S_0 for a

particular nonradiative transition. The values of S_0 were determined by using the values of p and $W_{NR}(0)$, shown in Figs. 3–6, and $N=1\times10^{13}$ s^{-1}. This value of N is based on the phonon energies and the sound velocities in ZBLA,[32] as well as previous determinations in other fluoride hosts.[33] As was found previously for Er^{3+} (Ref. 8), the values of S_0 for all fluorescent levels of Ho^{3+} are within the range 0.01–0.1. Thus, the values of $W_{NR}(0)$ are believed to be reasonable.

It has been shown that for rare-earth ions in solids, the multiphonon emission rate for a particular level has an exponential dependence on the energy gap to the next lower level.[8,10,17,18] This empirical "energy-gap law" is expressed as

$$W_{NR}=C\exp(-\alpha\Delta E)\,, \tag{16}$$

where C and α are positive constants characteristic of the host. This expression can not be used if the nonradiative transition is forbidden by selection rules or when one- or two-phonon processes are involved.[10] The values of these constants have been determined previously for ZBLA to be $C=1.88\times10^{10}$ s^{-1} and $\alpha=5.77\times10^{-3}$ cm.[8] In Fig. 10 the fitted low-temperature multiphonon emission rates for the various Ho^{3+} transitions (circles) are plotted semilogarithmically versus energy gap. Also shown are the values for several transitions of Er^{3+} (triangles) and the predicted values of W_{NR} (solid line) obtained by substituting the values of C and α for ZBLA in Eq. (16). The values found for Ho^{3+} are in agreement with these predicted values. This agreement is indicative that the values of W_{NR}, W_{ET}, and W_{rad} are indeed reasonable.

The phase-transition properties of glass are important and at this time not well understood. Recent work has been useful in pointing out the complexities in the crystallization behavior of fluorozirconate glass.[34–36] However, more information and new techniques are highly desirable. Figures 7 and 8 illustrate the potential for utilizing new methods to study devitrification. As shown in Fig. 8, there is a temperature-dependent incubation time for the crystallization of ZBLA glass. The latter stage of the crystallization in isothermal heating can be described by the equation

$$A_x=A_0[1-\exp(-kt)]\,, \tag{17}$$

where k is a constant. Our data suggest that the crystallization of ZBLA glass involves two distinct stages.

The existence of an incubation period for crystallization is well known, but not understood. A controlled atmosphere should be used if the observed incubation time is to be understood. In our sample, a surface cloudness associated with light scattering from crystallites was evident, initially followed by thermal deformation of the sample. The center of the sample remained glassly until near the end of the incubation time. This observation is consistent with the experimental results of Weinberg *et al.*[36] On the other hand, they have also shown that about 2×10^7 crystallites/cm^3 of 1-μm size are present in untreated ZBLA glass. The growth or multiplication of these initial crystallites could compete with surface crystallization. As described in the preceding section, devitrification changes the decay kinetics of $^4S_{3/2}$ of Er^{3+} ions from nearly single exponential to a single-exponential decay. This suggests that Er^{3+} ions in the devitrified host occupy a single site. Lucas *et al.*[4] showed that rare-earth ions substitute for network-forming ions (Zr and La) in ZBLA glass. The present result of the decay kinetics appears to be consistent with this idea. Obviously, a detailed study is needed.

V. CONCLUSIONS

It was shown recently that the radiative transition rates of Er^{3+} in ZBLA glass can be predicted accurately, by the Judd-Ofelt theory.[8] This technique has also been used for Ho^{3+} in the same host. The differences between the measured and radiative rates are attributed to two sources; multiphonon emission and energy transfer. The multiphonon emission rates were found to depend on the energy gap to the next lower level in the same manner as for ZBLA:Er.[8] The temperature dependence of the multiphonon emission rates were well described by single-frequency phonon models which have been used successfully.[8,10,17] The energy-transfer–rate temperature dependence can be described by a Boltzmann population-type expression.

The devitrification of ZBLA glass was studied by using rate-earth ions as probes. The glass undergoes rapid devitrification at a temperature near 630 K. After devitrification, the single-exponential decay of the fluorescence suggests that the rare-earth ion occupies a single type of site. This is in agreement with the conclusions of Lucas *et al.*[4]

ACKNOWLEDGMENTS

The authors would like to thank M. J. Weber for making available his values of the reduced matrix elements for Ho^{3+} in $YA1O_3$, and R. C. Powell for helpful discussion. This research was funded by U.S. Department of the Air Force Contract No. F-19628-83-K-0007.

[1]M. Poulain, M. Poulain, J. Lucas, and P. Brun, Mater. Res. Bull. **10**, 243 (1975).

[2]M. Poulain, M. Chanthanasinh, and J. Lucas, Mater. Res. Bull. **12**, 151 (1977).

[3]M. G. Drexhage, C. T. Moynihan, M. Saleh Boulos, and K. P. Quinlan, in *Proceedings of the Conference on the Physics of Fiber Optics,* edited by B. Bendow and S. S. Mitra (American Ceramic Society, Columbus, Ohio, 1981).

[4]J. Lucas, M. Chanthanasinh, M. Poulain, M. Poulain, P. Brun, and M. J. Weber, J. Non-Cryst. Solids **27**, 273 (1978).

[5]R. Reisfeld, E. Greenberg, R. N. Brown, M. G. Drexhage, and C. K. Jørgensen, Chem. Phys. Lett. **95**, 91 (1983).

[6]R. Reisfeld, G. Katz, N. Spector, C. K. Jørgensen, C. Jacoboni, and R. DePape, J. Solid State Chem. **41**, 253 (1982).

[7]R. Reisfeld, G. Katz, C. Jacoboni, R. DePape, M. G. Drexhage, R. N. Brown, and C. K. Jørgensen, J. Solid State Chem. **48**, 323 (1983).

[8]M. D. Shinn, W. A. Sibley, M. G. Drexhage, and R. N. Brown, Phys. Rev. B **27**, 6635 (1983).

[9]M. J. Weber, B. H. Matsinger, V. L. Donlan, and G. T. Surratt,

J. Chem. Phys. **57**, 562 (1972).
[10]M. J. Weber, Phys. Rev. B **8**, 54 (1973).
[11]N. Karayianis, D. E. Wortman, and H. P. Jenssen, J. Phys. Chem. Solids **37**, 675 (1976).
[12]R. Reisfeld, J. Hormadaly, and A. Muranevich, J. Non-Cryst. Solids **29**, 323 (1978).
[13]R. Reisfeld, A. Bornstein, J. Bodenheimer, and F. Flahaut, J. Lumin. **18/19**, 253 (1979).
[14]B. R. Judd, Phys. Rev. **127**, 750 (1962).
[15]G. S. Ofelt, J. Chem. Phys. **37**, 511 (1962).
[16]W. F. Krupke, Phys. Rev. **145**, 325 (1966).
[17]L. A. Riseberg and M. J. Weber, in *Progress in Optics,* edited by E. Wolf (Elsevier, New York, 1976), Vol. 14, p. 89.
[18]M. J. Weber, Phys. Rev. **157**, 262 (1967).
[19]B. G. Wybourne, *Spectroscopic Properties of Rare Earths* (Interscience, New York, 1965).
[20]Poor agreement between the fitted and measured oscillator strengths of the $^5G_5$ and $^3F_4$ absorption occurred when the matrix elements in Ref. 9 were used. Comparison with the matrix elements published by Carnall *et al.* [J. Chem. Phys. **49**, 4424 (1968)] showed considerable discrepancies only for those two levels. Good agreement was obtained by using the values of Carnall *et al.*
[21]M. J. Weber, T. E. Varitimos, and B. H. Matsinger, Phys. Rev. B **8**, 47 (1983).
[22]W. F. Krupke, IEEE J. Quantum Electron **QE-10**, 450 (1974).
[23]G. H. Dieke, *Spectra and Energy Levels of Rare Earth Ions in Crystals* (Interscience, New York, 1968).
[24]M. D. Shinn, J. C. Windscheif, D. K. Sardar, and W. A. Sibley, Phys. Rev. B **26**, 2371 (1982).
[25]D. L. Dexter, J. Chem. Phys. **21**, 836 (1953).
[26]R. Reisfeld, in *Structure and Bonding,* edited by J. D. Dunitz, P. Hemmerich, J. A. Ibers, C. K. Jørgenson, J. B. Neilands, R. S. Nyholm, D. Reinen, and R. P. J. Williams (Springer, New York, 1973), Vol. 13, p. 53.
[27]L. D. Merkle and R. C. Powell, Phys. Rev. B **20**, 75 (1979).
[28]L. A. Riseberg and H. W. Moss, Phys. Rev. **174**, 429 (1968).
[29]B. Bendow, P. K. Banerjee, M. G. Drexhage, J. Goltmann, S. S. Mitra, and C. T. Moynihan, Commun. Am. Ceram. Soc. **65**, C8 (1982).
[30]K. Huang and A. Rhys, Proc. R. Soc. London, Ser. A **204**, 406 (1950).
[31]W. H. Fonger and C. W. Struck, J. Lumin. **17**, 241 (1978).
[32]M. P. Brassington, T. U. Tailing, A. J. Miller, and G. A. Saunders, Mater. Res. Bull. **16**, 613 (1981).
[33]M. V. Iverson and W. A. Sibley, Phys. Rev. B **21**, 2522 (1980).
[34]J. Lucas, M. Chanthanasinh, M. Poulain, and M. Poulain, J. Non-Cryst. Solids **27**, 273 (1978).
[35]J. Zhonghong, H. Xinyuan, S. Xiuyu, and Z. Xiangshu, J. Non-Cryst. Solids **56**, 69 (1983).
[36]M. C. Weinberg, G. E. Neilson, and G. L. Smith, J. Non-Cryst. Solids **56**, 45 (1983).